The following publication H. Huang, A. V. Savkin and W. Ni, "Decentralized Navigation of a UAV Team for Collaborative Covert Eavesdropping on a Group of Mobile Ground Nodes," in IEEE Transactions on Automation Science and Engineering, vol. 19, no. 4, pp. 3932-3941, Oct. 2022 is available at https://dx.doi.org/10.1109/TASE.2021.3139590.

Decentralized Navigation of a UAV Team for Collaborative Covert Eavesdropping on a Group of Mobile Ground Nodes

Hailong Huang, Andrey V. Savkin and Wei Ni

***Abstract*—Unmanned aerial vehicles (UAVs) are increasingly applied to surveillance tasks, thanks to their excellent mobility and flexibility. Different from existing works using UAVs for video surveillance, this paper employs a UAV team to carry out collaborative radio surveillance on ground moving nodes and disguise the purpose of surveillance. We consider two aspects of disguise. The first is that the UAVs do not communicate with each other (or the ground nodes can notice), and each UAV plans its trajectory in a decentralized way. The other aspect of disguise is that the UAVs avoid being noticed by the nodes for which a metric quantifying the disguising performance is adopted. We present a new decentralized method for the online trajectory planning of the UAVs, which maximizes the disguising metric while maintaining uninterrupted surveillance and avoiding UAV collisions. Based on the model predictive control (MPC) technique, our method allows each UAV to separately estimate the locations of the UAVs and the ground nodes, and decide its trajectory accordingly. The impact of potential estimation errors is mitigated by incorporating the error bounds into the online trajectory planning, hence achieving a robust control of the trajectories. Computer-based simulation results demonstrate that the developed strategy ensures the surveillance requirement without losing disguising performance, and outperforms existing alternatives.**

***Note to Practitioners*—The paper is motivated by the covertness requirement in the radio surveillance (also called eavesdropping) by UAVs. In some situations, the UAV user (such as the police department) wishes to disguise the surveillance intention from the targets, and the trajectories of UAVs play a significant role in the disguising. However, the typical UAV trajectories such as standoff tracking and orbiting can easily be noticed by the targets. Considering this gap, we focus on how to plan the UAVs' trajectories so that they are less noticeable while conducting effective eavesdropping. We formulate a path planning problem aiming at maximizing a disguising metric, which measures the magnitude of the relative position change between a UAV and a target. A decentralized method is proposed for the online trajectory planning of the UAVs based on MPC, and its robust version is also presented to account for the uncertainty in the estimation and prediction of the nodes' states.**

***Index Terms*—Wireless communications, radio surveillance, model predictive control (MPC), decentralized control, unmanned aerial vehicles (UAVs), trajectory planning.**

This work received funding from the Australian Government, via grant AUSMURIB000001 associated with ONR MURI grant N00014-19-1-2571. It is also supported by Australian Research Council and PolyU start-up fund under Project P0038447.

H. Huang is with the Department of Aeronautical and Aviation Engineering, the Hong Kong Polytechnic University, Hong Kong. (E-mail: hailong.huang@polyu.edu.hk).

A.V. Savkin is with School of Electrical Engineering and Telecommunications, University of New South Wales, Sydney 2052, Australia. (E-mail: a.savkin@unsw.edu.au).

Wei Ni is with Data61, CSIRO, Australia. (E-mail: wei.ni@data61.csiro.au).

I. Introduction

Unmanned Aerial Vehicles (UAVs) have found various applications, including but not limited to area surveillance, parcel delivery and agriculture [1]–[4], due to the decreasing cost of UAVs and their excellent mobility. Many publications have investigated the different roles of UAVs in wireless communications. In most cases, UAVs play the role of base stations in the air and provide wireless communication service [5]–[7], well-positioned to provide a high quality of service for cellular users. Some publications investigate other functions of UAVs, such as relays to provide connectivity in remote areas or gather sensory data from IoT devices.

Besides aerial base stations, UAVs can also protect wireless communications. There are two popular scenarios on this topic. In the first scenario, a UAV transmits data with a ground node when an eavesdropper is present. By optimally placing the UAV, the reference [8] maximizes the secrecy capacity of the UAV-node link. To optimize the average secrecy rate over a period, the papers [9], [10] present methods by optimizing the UAV's trajectory as well as the transmission power jointly. The paper [11] derives the outage probability of the receiver and the interception probability of the eavesdropper, followed by optimizing the UAV deployment and jamming power accordingly. An IoT device is considered to send data to a hovering UAV in [12], and a friendly UAV protects the transmission by jamming nearby eavesdroppers. The cumulative distribution functions are derived for the signal-to-interference-plus-noise ratio (SINR) of the legitimate and eavesdropping links. Analytical expressions are established for the secrecy outage probability and the average secrecy rate. The paper [13] considers a system comprising a transmitter, a receiver, a UAV relay and an eavesdropper. To prevent eavesdropping, an optimization problem of maximizing the system secrecy rate is studied where the transmission powers of the transmitter and the UAV are optimized.

In the second scenario, a UAV functions as a jammer to confuse eavesdroppers [14], [15]. The paper [16] jointly optimizes the UAV's trajectory and the jamming power for maximizing the average secrecy rate. The papers [17] and [18] propose schemes with two UAVs: while the first UAV transmits useful messages, the second UAV broadcasts jamming signals. The UAVs' trajectories and the transmission powers, and the user schedule are optimized jointly. The paper [19] considers that two UAVs send confidential messages to their respective ground destinations using the same spectrum. The authors

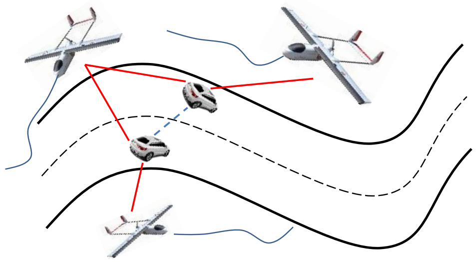

Fig. 1: The considered scenario of using a UAV team to conduct radio surveillance on mobile targets.

design a cooperation strategy to combat eavesdropping.

This paper presents a new online aeronautic control of the trajectories for a UAV team that launches the radio surveillance on a group of suspicious ground moving targets in a cooperative and uncommunicative way; see Fig. 1. While effectively capturing the wireless transmissions of the ground nodes, the UAVs hide their surveillance intention. A metric quantifying the visual disguising performance is adopted, which is based on the UAV-target relative angle and distance [20]. The online control of the UAV trajectories is formulated to optimize the overall disguising metric, and a radio surveillance requirement, the collision avoidance, and UAVs' aeronautic manoeuvrability are considered as constraints. Given the dynamic nature of this online control problem, a model predictive control (MPC)-based technique is presented, allowing each UAV to predict the other UAVs' and the targets' movements and decide its next move in real-time. The prediction errors' influence is mitigated by exploiting MPC's online adjustability and integrating the error bounds in the control, which lead to the robust control of the trajectories in a decentralized manner. We conduct extensive computer simulations and compare with a randomized method. The results reveal that the developed approach satisfies the radio surveillance requirement while not sacrificing the disguising intention.

To the best of our knowledge, our considered scenario has not been investigated. Existing approaches optimize an integrated securing performance over a certain period, e.g., [9], [10], [16]; explore the random movements of UAVs, e.g., [21]; or allow sharp turns and only suit for particular types of UAVs, e.g., [19]. Moreover, stationary ground nodes are typically considered in the literature. In contrast, this paper considers a nonlinear motion model accounting for the aeronautic manoeuvrability of the UAVs. In particular, we focus on covert radio surveillance which significantly distinguishes from the existing studies. The UAVs need to make an effort to hide their surveillance intention and construct their trajectories in a decentralized manner. We consider radio surveillance with wireless channel models incorporated, and this is different from the well-studied UAV-based video surveillance, where a disk area often represents the coverage area [22]. All these new considerations make the problem under consideration practical and challenging. This paper falls into the group of model-based approaches. Data-based approaches using machine learning techniques, such as deep reinforcement learning (DRL), can also be used for UAV trajectory planning [23]. The problem of interest can be considered as a multi-agent Markov decision process (MDP) and potentially solved using multi-agent DRL. However, the design and training of multi-agent DRL are non-trivial. One reason is that there are multiple targets moving along unknown trajectories. The distances between the targets and the monitors keep changing randomly. It is non-trivial to confirm the existence of an equilibrium of the multi-agent DRL, e.g., by using game theory. In other words, it is challenging to design the reward or penalty, or train the multi-agent DRL to converge. Another reason is that large and representative datasets are needed for the design, training and generalization of learning approaches The UAVs may already fail (e.g., fail the eavesdropping mission, be noticed by targets, fall, or collide) before their learning models converge if they can converge.

In our recent work [24], the navigation problem of a UAV for securing the communication with a stationary or moving ground target is studied in the presence of eavesdroppers. In another work [25], the scenario of using a fleet of UAVs to conduct eavesdropping on a set of stationary targets is studied, and a Rapidly-exploring Random Tree (RRT)-based centralized scheme is proposed. The algorithms developed in [24] and [25] cannot be applied to the problem studied in this paper, where we consider a new and distinctively different scenario of fully decentralized covert radio surveillance on a group of moving targets by a UAV team. An initial study of this new scenario was conducted under the ideal assumption of the error-free estimation and prediction of targets' trajectories, and primary results are published in [26]. Compared to [26], this paper presents a more holistic analysis of new scenario by considering the practical situation with the non-negligible state estimation and prediction errors. In particular, we construct new constraints to guarantee the safe operation of the UAV team and the effectiveness of their radio surveillance by incorporating the bounds of errors. Additionally, more comprehensive simulations are conducted in this paper, including the computing efficiency analysis and scalability of the proposed algorithm under estimation and prediction errors.

The rest of this paper is organized as follows. Section II presents the system model and states the considered problem. Section III presents the MPC-based trajectory planning method and then discusses how to use it to deal with the expected system uncertainty. Computer simulations are presented in Section IV to validate and evaluate the proposed approach. A conclusion is drawn in Section V finally.

II. Problem Statement

We consider that there are $\mathcal{N}$ UAVs collaboratively eavesdrop on the communications among $\mathcal{M}$ moving nodes on the ground. TABLE I summarizes the frequently used symbols in the paper.

Denote $p_i(t) = [x_i(t), y_i(t), z_i(t)]$ as UAV i's position ($i =$

TABLE I: Mainly used symbols and the meanings

Symbol	Meaning
p_i	The position of UAV i
θ_i	The flight path angle of UAV i
μ_i	The flight path angle rate of UAV i
ψ_i	The heading angle of UAV i
ϕ_i	The bank angle of UAV i
v_i	The speed of UAV i
q_j	The position of node j
d_{ij}	Distance from UAV i to node j
δ_{ih}	Distance from UAVs i to h
γ_{ij}	Relative angle between UAV i and node j
h_{ij}	Channel coefficient from UAV i to node j
SNR_{ij}	SNR at UAV i from node j
F_j	The combined SNR from node j
g_{ij}	Disguising performance of UAV i to node j
S_i	Average distance threshold for UAV i
S_0	The minimum distance between two UAVs
$\hat{p}_{h(i)}$	Position of UAV h estimated at UAV i
$\hat{p}_{j(i)}$	Position of node j estimated at UAV i
Δ^n_{ij}	Error bound of node j estimated at UAV i
Δ^u_{ij}	Error bound of UAV h estimated at UAV i
P	Transmit power of nodes
$\mathcal{N}$	The number of UAVs
$\mathcal{M}$	The number of target nodes
$\mathcal{T}$	Optimization horizon
$\mathcal{L}$	Number of slots of one optimization horizon

$1, \ldots, \mathcal{N}$) at time t. The motion of UAVs is modelled by [27]:

$$\begin{cases} \dot{x}_i = v_i \cos\theta_i \cos\psi_i, \\ \dot{y}_i = v_i \cos\theta_i \sin\psi_i, \\ \dot{z}_i = v_i \sin\theta_i, \\ \dot{\theta} = \mu_i, \\ \dot{\psi} = \frac{g \tan\phi_i}{V_i}, \end{cases} \tag{1}$$

where v_i is the speed of UAV i, θ_i is the flight path angle, μ_i denotes the flight path angle rate, ψ_i denotes the heading angle, and ϕ_i is the bank angle. The state of the model (1) is $\{p_i, \theta_i, \psi_i\}$, and the control input is $\{v_i, \mu_i, \phi_i\}$. v_i, μ_i and ϕ_i satisfy that $|v_i| \leq V_i^{max}$, $|\mu_i| \leq U_i^{max}$ and $|\phi_i| \leq \Phi_i^{max}$, where V_i^{max}, U_i^{max} and Φ_i^{max} are given constants depending on the maneuverability of UAV i. Each UAV i needs to operate within a certain range of altitude:

$$Z^{min} \leq z_i(t) \leq Z^{max}, \tag{2}$$

where the allowed range $[Z^{min}, Z^{max}]$ is known.

Let $q_j(t) = [x'_j(t), y'_j(t), 0]$ ($j = 1, \ldots, \mathcal{M}$) denote node j's location at t. As assumed in [8], [10], a UAV can estimate other UAVs' and ground nodes' positions using onboard cameras. Also assume that the nodes' movements can be predicted for a certain time period in the future. We start with accurate predictions in this section and then extend to predictions with errors in the next section.

Denote $d_{ij}(t)$ as the Euclidean distance from UAV i to node j at t:

$$d_{ij}(t) = \|p_i(t) - q_j(t)\|, \tag{3}$$

where $\|\cdot\|$ gives 2-norm. Let $h_{ij}(t)$ be the complex channel coefficient from node j to UAV i at t, and it can be measured at the UAV. The channels between UAVs and nodes are line-of-sight dominated, and they enable UAVs to outperform the ground eavesdroppers [28]. With this assumption, $h_{ij}(t)$ follows the free-space path loss model:

$$h_{ij}(t) = \frac{P_0}{d_{ij}^a(t)}, \tag{4}$$

where P_0 is the reference transmit power of a node at the distance of 1 meter and a is the path loss exponent. The Doppler effect caused by the UAV's and node's movements is assumed to be well compensated at the UAV.

Moreover, denote P as the transmission power of the nodes and σ_0^2 as the noise power at UAVs. The signal-to-noise ratio (SNR) at UAV i from node j is given by

$$\text{SNR}_{ij}(t) = \frac{P h_{ij}(t)}{\sigma_0^2}. \tag{5}$$

Maximum ratio combining is conducted to combine constructively the captured signals of all UAVs for the maximum combined SNR [24]. The combined instantaneous SNR of the collaborative radio surveillance in regards to node j is written as

$$F_j(t) = \sum_{i=1}^{\mathcal{N}} \text{SNR}_{ij}(t). \tag{6}$$

Assume that no useful information is extractable from collected data if $F_j(t)$ is lower than a certain threshold C. Then, the below constraint should be met to ensure that the data gathered by the UAV team at t is useful:

$$F_j(t) \geq C, \ \forall j. \tag{7}$$

Here, the threshold C can be specified based on the known highest modulation-and-coding and coding order of the ground nodes. It is pointed out that when the UAVs are executing the covert radio surveillance, they do not exchange the received data with each other. Instead, the collected signals are combined and decoded only after the mission.

Remark II.1. *Constraint (7) requires the UAV team to have effective radio surveillance on all the ground nodes at any time. In the cases when the transmission schedule is available to the UAV team, we can introduce a new notation $s_j(t)$ to indicate the transmission schedule for node j at time t: $s_j(t) = 1$ if it transmits; $s_j(t) = 0$, otherwise. Then, (7) becomes $F_j(t) \geq C s_j(t)$, $\forall j$, $\forall t$. This will significantly reduce the restrictions on the UAVs' movements. Thus, though out of the scope of this paper, observing the transmission pattern via some machine learning algorithms is an interesting future research direction under the considered context.*

When multiple UAVs collaborate, collision avoidance should be considered. Denote S_0 as a safety distance. Let $\delta_{ih}(t)$, which is computed by $\delta_{ih}(t) = \|p_i(t) - p_h(t)\|$, be the relative distance from UAV i to UAV h at t. Any two UAVs must stay S_0 away from each other at t:

$$\delta_{ih}(t) \geq S_0, \forall i \neq h, \tag{8}$$

Moreover, to hide the surveillance intention, the UAVs need to keep away from the nodes. The main reason is the

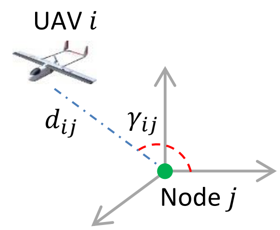

Fig. 2: Illustration of several key symbols.

observation that staying closer to a target makes the UAV more suspicious. Considering this, the below constraint is used:

$$\frac{1}{\mathcal{T}} \int_{t_k}^{t_k+\mathcal{T}} d_{ij}(t)dt \geq S_i, \ \forall j, \ \forall i, \tag{9}$$

where t_k is an instant and S_i is used to characterize the average distance between a UAV and a node during a period of $\mathcal{T}$. The value of S_i is dependent on the dimensions of UAV i. Generally speaking, a small-size UAV i corresponds to a small S_i, because a small object is less noticeable than a large one. The period $\mathcal{T}$ is comparatively short in regards to the whole mission time. The location of a node is assumed to be predictable for the upcoming period of $\mathcal{T}$.

Staying at some positions S_i away from a node on average, i.e., the condition (9), may not be sufficient to conceal the monitoring intent. We wish the UAVs to move in a random-like manner since a random movement is a reasonable way to disguise. Denote $\gamma_{ij}(t)$ as the relative angle of UAV i and node j, measured counter-clockwisely from a fixed direction (such as the x-axis) to the straight line connecting the UAV and the node; see Fig. 2. The disguising metric is measured by the weighted amplitudes of the first-order derivatives of the relative angle and distance of the UAV and the node [20]:

$$g_{ij}(t) = \kappa|\dot{\gamma}_{ij}(t)| + |\dot{d}_{ij}(t)|. \tag{10}$$

Here, κ is a positive weighting factor. The rationale of (10) is that, when we look at some object, if the object moves in very different directions with significant displacements relative to us, it seems not to monitor us. A comparison of the disguising performance of some movement patterns of straight line, arc and random movement on a 2D plane is given in Fig. 3a. The starting positions and the linear speeds are the same across these movements. An observer keeps measuring the relative distance and angle from the object to itself. For the random pattern, the object randomly turns left, right or moves forward. From common sense, moving randomly helps to hide intention, and the results of the disguising performance under the considered metric (10) in Fig. 3b aligns with this observation. Therefore, the proposed metric (10) is reasonable. Additionally, the value of κ significantly influences the movements of the UAVs. In particular, when κ takes some large value, the UAVs prefer to change the relative angle with respect to the targets. When κ takes some small value, the UAVs prefer to change the relative distance with respect to the targets. The selection of κ should be based on field experiments with the participation of volunteers, i.e., how the

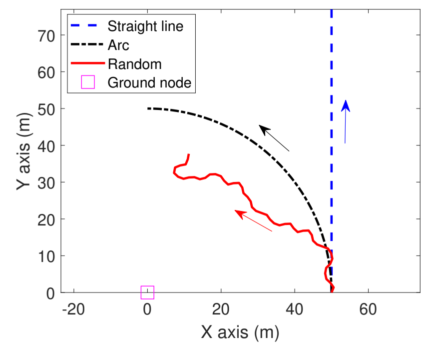

(a)

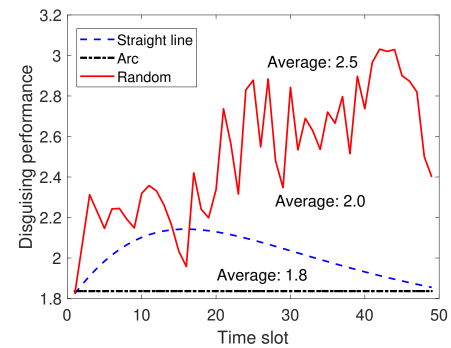

(b)

Fig. 3: Evaluation of the disguising metric (10). (a) Trajectories of an object moving along a straight line, an arc, and randomly on a 2D plane. (b) The results of the disguising metric corresponding to the movements in (a).

volunteers feel about the change of the relative distance and relative angle. In this paper, we set κ as a fixed value and leave the study on the value selection for further investigation. It is worth noting that the metric (10) is just one option to describe the disguising performance. As will be seen in the next section, the developed method is not restricted to this model.

We consider the below function for maximizing the overall disguising metric:

$$\max_{p_1(t),\ldots,p_{\mathcal{N}}(t)} \sum_{i=1}^{\mathcal{N}} \sum_{j=1}^{\mathcal{M}} \frac{1}{S_i} \int_{t_k}^{t_k+\mathcal{T}} (\kappa|\dot{\gamma}_{ij}(t)| + |\dot{d}_{ij}(t)|)dt. \tag{11}$$

In (11), a small-size UAV can make less effort in disguising itself than a large-size UAV, because the latter is more detectable. In the case where the UAVs are of the same size, we omit the weights. The current formulation does not consider the energy consumption, as the fixed-wing UAVs modelled by (1) is typically much more energy-efficient and can fly for a much longer time than rotary-wing UAVs [29]. Nevertheless, we note that energy consumption is important to trajectory planning, especially when the operation time increases. To capture this factor, we can potentially extend the current optimization problem with a single objective function to a multi-objective optimization problem. In addition to the currently considered disguising metric, another metric describing the energy consumption of the UAVs, such as the length of UAVs'

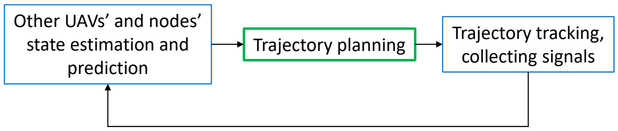

Fig. 4: The estimate-predict-plan-calibrate working manner of each UAV of the team.

trajectories and the magnitudes of the UAVs' control inputs, can be considered as the second objective function.

Given that a team of UAVs are able detect the coordinates of an object and predict its position for a future period $\mathcal{T}$, and given the constants C, S_0, S_i, $V_i^{\max}$, $U_i^{\max}$ and $W_i^{\max}$ ($i = 1, \ldots, \mathcal{N}$), we restrict out attention to maximize (11) in a decentralized manner while satisfying constraints (2), (7), (8) and (9).

III. Proposed Method

Problem (11) subject to (2), (7), (8) and (9) is difficult as it does not provide the analytical solution. In (11), $\dot{\gamma}_{ij}(t)$ is non-convex with respect to $v_i(t), u_i(t), \omega_i(t)$, so as $\dot{d}_{ij}(t)$. The absolute value operator further results in that they are not differentiable at the point of zero. In addition, the control commands $v_i(t), u_i(t), \omega_i(t)$ for each UAV lead to a solution space in the size of $O(3^{\mathcal{N}})$ under the condition that they keep unchanged during an interval. However, remaining the same may make it probable for the ground nodes to notice the UAVs' intention. Thus, $v_i(t)$, $u_i(t)$ and $w_i(t)$ should vary in $[t_k, t_k + \mathcal{T}]$ to achieve a good disguise. The necessity of reserving a large solution space complicates the problem.

We present an MPC-based decentralized UAV trajectory planning scheme. We first consider the scenario where the estimations and predictions of the nodes' and UAVs' movements are accurate and present the basic MPC-based trajectory planning method in Section III-A. We then consider the practical case with estimation and prediction errors and exploit the error bounds to design a robust trajectory planning method in Section III-B. We only discuss how UAV i plans its trajectory, and other UAVs can do it in the same way.

A. MPC-based trajectory optimization

We assume that each UAV carries some sensors such as cameras to measure the states of other UAVs and ground nodes. Also, each UAV can make predictions on the ground nodes' movements. With the measurements, the state estimation can be conducted by existing approaches, e.g., extended Kalman filter [30]. The working manner of each UAV of the team is shown in Fig. 4.

The interval $\mathcal{T}$ (the horizon during which the trajectories are planned) is divided by a constant τ into $\mathcal{L}$ ($\mathcal{L} = \lfloor \frac{\mathcal{T}}{\tau} \rfloor$) slots. The control commands $v_i(t)$, $u_i(t)$ and $w_i(t)$ are assumed to update only at instants $t_k, t_k + \tau, \ldots, t_k + (\mathcal{L} - 1)\tau$ and do not change during the slots $[t_k + l\tau, t_k + (l+1)\tau]$, $l = 0, 1, \ldots, \mathcal{L} - 1$. With such discretized time slots, constraints (2), (7) and (8) are rewritten in discrete forms. Specifically, we assess the constraints only at instants $t_k, t_k + \tau, \ldots, t_k + (\mathcal{L} - 1)\tau$, rather than in the continuous-time domain. Then, constraint (9) becomes:

$$\frac{1}{\mathcal{L}} \sum_{l=1}^{\mathcal{L}} d_{hj}(t_k + l\tau) \geq S_h, \forall j, \forall h. \tag{12}$$

The objective function is re-written in the discretized form:

$$\begin{aligned} &\max_{p_1(t_k+l\tau), \ldots, p_{\mathcal{N}}(t_k+l\tau)} \sum_{h=1}^{\mathcal{N}} \sum_{j=1}^{\mathcal{M}} \sum_{l=1}^{\mathcal{L}} \\ &\frac{1}{S_h}(\kappa|\gamma_{hj}(t_k + l\tau) - \gamma_{hj}(t_k + (l-1)\tau)| + \\ &\qquad |d_{hj}(t_k + l\tau) - d_{hj}(t_k + (l-1)\tau)|). \end{aligned} \tag{13}$$

Denote n_v, n_μ and n_ϕ as some given positive integers. They determine the numbers of feasible control inputs at each slot in the below class:

$$\begin{aligned} v_i &= \frac{s_v V_i^{max}}{n_v} && \forall s_v = 1, \ldots, n_v, \\ \mu_i &= \frac{s_\mu U_i^{max}}{n_\mu} && \forall s_\mu = -n_\mu, \ldots, -1, 0, 1, \ldots, n_\mu, \\ \phi_i &= \frac{s_\phi \Phi_i^{max}}{n_\phi} && \forall s_\phi = -n_\phi, \ldots, -1, 0, 1 \ldots, n_\phi. \end{aligned} \tag{14}$$

In (14), there are n_v choices for v_i, $(2n_\mu + 1)$ choices for μ_i, and $(2n_\phi + 1)$ choices for ϕ_i. So, there are $n_v(2n_\mu + 1)(2n_\phi + 1)$ sets of possible control inputs at each slot. Then, there are $(n_v(2n_\mu + 1)(2n_\phi + 1))^{\mathcal{L}}$ possible control sequences for $\mathcal{L}$ slots.

In this paper, we adopt the MPC framework to construct UAVs' trajectories. Some concepts used in the proposed algorithm are explained as follows:

- The set of control commands v_i, μ_i and ϕ_i from (14) is called **a set of control commands** at t for UAV i.
- The $\mathcal{L}$ sets of control commands that will be applied at any UAV at $t_k, t_k + \tau, \ldots, t_k + (\mathcal{L} - 1)\tau$ is called **a control sequence**.
- The set of $\mathcal{N}$ control sequences for $\mathcal{N}$ UAVs is called **a combination of control sequences**.

The UAV team commences the collaborative surveillance at t_0. UAV i constructs its trajectory using the below procedures at $t_k = k\tau$ for $k = 0, 1, 2, \ldots$.

S1: 1) Estimate the locations and headings of the other UAVs, as well as the locations and speeds of the ground nodes, and 2) forecast the nodes' positions for the upcoming $\mathcal{L}$ slots based on the estimations.

S2: Consider all possible control commands from (14) and apply them to the UAVs at $t_k, t_k + \tau, \ldots, t_k + (\mathcal{L} - 1)\tau$. This will create multiple trajectories of the UAVs.

S3: Choose the combination of control sequences maximizing (13) and satisfying (2), (7), (8) and (12) at $t_k + \tau, \ldots, t_k + \mathcal{L}\tau$. The first combination will be chosen when two or more combinations of control sequences give the same objective value of (13).

S4: Implement the first set of control commands of the ith control sequence.

Proposition III.1. *The global maximum of problem (13) subject to (2), (7), (8) and (12) exists. With* $n_v \to \infty, n_\mu \to$

$\infty, n_\phi \to \infty$ and $\mathcal{L} \to \infty$, the control sequence obtained in **S2** *and* **S3** *converges to the global optimum.*

Proof. From the model (1) we understand that the trajectories $(x_i(\cdot), y_i(\cdot), z_i(\cdot))$ for $i = 1, \ldots, \mathcal{N}$ under constraints (2), (7), (8) and (12) are continuous and bounded uniformly [31]. Thus, these trajectories are compact following the Arzela–Ascoli theorem, and the global maximum of the problem (13) can be achieved at some trajectory $(x_i^*(\cdot), y_i^*(\cdot), z_i^*(\cdot))$ [31]. Moreover, the control inputs $(v_i^*(\cdot), \mu_i^*(\cdot), \phi_i^*(\cdot))$ that lead to the optimal trajectory can be approximated by a piecewise constant function with an arbitrary small precision. In other words, with $n_v \to \infty, n_\mu \to \infty, n_\phi \to \infty$ and $\mathcal{L} \to \infty$, the control sequence obtained in **S2** and **S3** converges to $(v_i^*(\cdot), \mu_i^*(\cdot), \phi_i^*(\cdot))$. This completes the proof of Proposition III.1. □

When the UAVs and ground nodes' positions are measured precisely, different UAVs get the unique combination of control sequences following the above procedures. In other words, each UAV addresses the considered problem and executes the first set of control commands in the control sequence belonging to itself. This set of control commands leads the UAV to a new position, at which it repeats the procedures.

We note that the position estimations by a UAV may be inaccurate in practice. In this sense, the result of the proposed method serves as an asymptotic upper bound. One way to reduce the errors' impact is the introduction of a fading factor. In particular, a given constant $\lambda \in (0, 1)$ can be introduced, and λ^l can be multiplied by the contribution at each instant $t_k + l\tau$ in (13).

We also note that the proposed MPC-based scheme repeatedly optimizes the considered problem in a smaller time window $\mathcal{T}$ than the whole horizon. In this sense, the proposed scheme falls behind some other optimization algorithms such as Linear-Quadratic Regulator (LQR) [32] which optimizes the entire horizon. Compared to LQR (which can obtain the optimal solution), the proposed MPC-based algorithm may obtain a suboptimal solution. However, the proposed method can be implemented online and can adjust the control commands actively upon the latest measurements, which is more suitable for time-variant problems. In addition, the proposed method can handle the nonlinear constraint (7) and the nonlinear objective function (13) without linearization.

Now, we provide more details on the trajectory searching strategies applied in **S3**. Without any constraint, each UAV searches its trajectory in the complete tree. With the consideration of (2), (7), (8) and (12), the tree to be searched can be significantly reduced. Our searching strategy firstly removes all the vertices whose altitudes are outside the range of $[Z_{min}, Z_{max}]$ from the tree (i.e., the positions that violate constraint (2)). Their child vertices are also removed from the tree. Secondly, the trajectories whose average distances to the ground nodes are smaller than the given threshold (i.e., the trajectories that violate constraint (12)) are removed from the tree. Thirdly, we consider constraint (8) for collision avoidance. When a vertex of a tree is within a S_0 distance of a vertex of another tree, one of these two vertices is removed. The rule is to remove the vertex in the tree with more vertices. This rule helps balance the number of vertices in the trees of the UAVs. With these operations, the number of feasible trajectories is reduced significantly. Finally, we verify constraint (7) for each feasible trajectory combination. If constraint (7) holds, we record the objective function value of (13). By doing this, we can find out the best trajectory combination.

B. Robust trajectory optimization

In practice, the estimations may not be perfect. Moreover, the estimation errors cannot be known in real-time. To eliminate the impact of the estimation errors on trajectory planning, we take them into account in trajectory optimization. In this subsection, we present a robust form of the proposed MPC-based trajectory optimization method.

Let $\hat{p}_{h(i)}(t)$ and $\hat{q}_{j(i)}(t)$ stand for the positions of UAV h and node j estimated by UAV i at t, respectively. Assume that the estimation errors are random variables and are bounded. We have

$$\|p_{h(i)}(t) - \hat{p}_{h(i)}(t)\| \leq \Delta_{ih}^u, \tag{15}$$

$$\|q_{j(i)}(t) - \hat{q}_{j(i)}(t)\| \leq \Delta_{ij}^n, \tag{16}$$

where $\Delta_{ih}^u > 0$ and $\Delta_{ij}^n > 0$ limit the errors of the UAV i's estimated positions of UAV h and node j, respectively. In practice, Δ_{ih}^u and Δ_{ij}^n depend on the resolution of the cameras mounted on UAV i. Suppose that UAV i can reject some disturbance, such as wind, which enables the UAV to know its position perfectly. Thus, we have $\Delta_{ii}^u = 0$. We assume that the bounds are known to UAV i and they are considered in the trajectory optimization.

To accommodate the estimation errors, we rewrite the worst-case constraints (2), (7), (8) and (9) as follows:

$$Z^{min} + \Delta_{ih}^u \leq z_h(t_k + l\tau) \leq Z^{max} - \Delta_{ih}^u, \forall h, \forall l, \tag{17}$$

$$\sum_{h=1}^{\mathcal{N}} f(d_{hj}(t_k + l\tau) + \Delta_{ih}^u + \Delta_{ij}^n) \geq C, \forall j, \forall l, \tag{18}$$

$$\delta_{ih}(t_k + l\tau) \geq S_0 + \Delta_{ih}^u, \forall i \neq h, \forall l, \tag{19}$$

$$\frac{1}{\mathcal{L}} \sum_{l=1}^{\mathcal{L}} d_{hj}(t_k + l\tau) \geq S_h + \Delta_{ih}^u + \Delta_{ij}^n, \forall j, \forall h. \tag{20}$$

Constraint (17) narrows down the range of the allowed altitude. Constraint (18) specifies the collaborative radio surveillance requirement. UAV i needs to further estimate the distance from UAV h to node j. In the worst case, the estimation error of the distance is $\Delta_{ih}^u + \Delta_{ij}^n$. Constraint (19) enlarges the safety distance between UAVs i and h by a margin specified by the estimation error bound Δ_{ih}^u. Constraint (12) increases the required average distance between UAV h and node j by a margin $\Delta_{ih}^u + \Delta_{ij}^n$. Clearly, if the UAVs are at positions satisfying (17), (18), (19) and (20), the original constraints (2), (7), (8) and (9) hold as well. In this sense, these new constraints are tightened by the error bounds, and provide the robust versions of the original constraints [33]. We note that larger bounds increase the robustness to the estimation errors, but excessively large bounds can make the problem infeasible.

Therefore, the considered optimization problem becomes maximizing (13) subject to (17), (18), (19) and (20). The MPC-based trajectory optimization method proposed in Section III-A can be applied to address the new problem by replacing constraints (2), (7), (8) and (12) in **S3** with (17), (18), (19) and (20). We note that the robust versions of the constraints may lose the optimality of the original problem because the feasible solution space is reduced. In addition, since the UAVs solve the problem in a decentralized way, the trajectory of UAV h constructed by UAV i can be different from the trajectory constructed by UAV h itself. The reason lies in the estimation error of the position of UAV h at UAV i. Despite solving the robust version optimization problem may penalize disguising performance, nonetheless, none of the original constraints is violated, which guarantees the safe operation of the UAV team and the effectiveness of the radio surveillance during the mission. In the next section, we will show via extensive computer simulations that though different UAVs may obtain different sets of trajectories, the disguising performance is negligibly impacted.

IV. Performance Evaluation

This section evaluates the developed approach via computer simulations. First, we provide the theoretical complexity and scalability of the overall framework.

A. Theoretical complexity and scalability analysis

We study the complexity and scalability of the proposed algorithm, subject to the numbers of UAVs and mobile nodes, i.e., $\mathcal{N}$ and $\mathcal{M}$. In **S1**, each UAV estimates the locations and headings of other $(\mathcal{N}-1)$ UAVs and the locations and speeds of $\mathcal{M}$ target nodes. Using these estimations, it further predicts the nodes' positions for future $\mathcal{L}$ slots. Thus, the number of computations required is $O(\mathcal{N}-1+\mathcal{M}(\mathcal{L}+1)) = O(\mathcal{N}+\mathcal{M}\mathcal{L})$. Furthermore, the number of possible control commands from (14) for each UAV is $(n_v(2n_\mu+1)(2n_\phi+1))^{\mathcal{L}}$. Since the proposed algorithm is decentralized, at each UAV i, the computations require calculating future trajectories of all $\mathcal{N}$ UAVs. Therefore, the total number of control inputs considered at each UAV is $(n_v(2n_\mu+1)(2n_\phi+1))^{\mathcal{L}\mathcal{N}}$. Moreover, the amount of computations required by (12) depends linearly on $\mathcal{M}$. Hence, the amount of computations required in **S2, S3** and **S4** is $O(\mathcal{M}(n_v(2n_\mu+1)(2n_\phi+1))^{\mathcal{L}\mathcal{N}})$. The total amount of computations required by the algorithm is $O(\mathcal{N}+\mathcal{M}\mathcal{L})+O(\mathcal{M}(n_v(2n_\mu+1)(2n_\phi+1))^{\mathcal{L}\mathcal{N}})$. Consider fixed $\mathcal{L}, n_v, n_\mu$ and n_ϕ and analyze the complexity in regards to $\mathcal{N}$ and $\mathcal{M}$. Given fixed $\mathcal{N}$, the amount of computations is approximately linear to $\mathcal{M}$. Given fixed $\mathcal{M}$, the number of computations increases exponentially with $\mathcal{N}$. Hence, the proposed algorithm can readily scale with the number of mobile ground nodes $\mathcal{M}$. Moreover, the number of UAVs $\mathcal{N}$ is typically moderate and the subsequent computations are manageable in practice.

B. Computer simulations

Now, we present computer simulation results to verify the effectiveness of the developed approach. We first present a case with three nodes following a curvy trajectory. There are two UAVs conducting the surveillance mission. They apply the developed method to construct trajectories. The simulation lasts 90 slots with 20 seconds per slot. Other system parameters are: $\mathcal{L}=3$, $\tau=1$, $Z^{min}=60$ m, $Z^{max}=240$ m, $P=20$ dBm, $\sigma_0^2=-80$ dBm, $P_0=-50$ dB $a=3$, $C=5$ dB, $\kappa=100$, $S_0=100$ m, $S_1=160$ m, $S_2=140$ m, $V^{max}=30$ m/s, $U^{max}=1$ rad/s, $\Phi^{max}=0.5$ rad, $n_v=1$, $n_\mu=1$, $n_\phi=1$, $\Delta_{12}^u=10$ m, $\Delta_{21}^u=20$ m, $\Delta_{11}^n=20$ m, $\Delta_{12}^n=20$ m, $\Delta_{21}^n=30$ m, $\Delta_{22}^n=30$m, $\Delta_{13}^n=20$ m and $\Delta_{23}^n=20$ m. At each slot, we randomly create the errors of the estimation in the bounds, and the errors are integrated into the actual locations of the UAVs and ground nodes.

The UAVs' movements are displayed in Figs. 5a and 5b when the error bounds are not considered. The trajectories of the UAVs take into account the estimation error bounds in Figs. 5c and 5d. Clearly, due to the estimation errors, the UAVs can construct different trajectories. Since no other references study the considered problem, a randomized method is regarded as a baseline. Specifically, this baseline addresses the purpose of disguise by only randomly selecting a set of control commands from (14). The 3D trajectories are demonstrated separately in Fig. 5e with the horizontal trajectory and in Fig. 5f with the altitude. The performance of the radio surveillance is shown in Fig. 5g under the three sets of trajectories. In this figure, only the lower value of the radio eavesdropping achievement of the ground nodes at each instant is presented. Clearly, due to the estimation errors, the collaborative radio surveillance requirement is violated several times when the errors are not accounted for in the trajectory construction. The random method fails to ensure the surveillance requirement. Differently, the developed method with error bounds results in effective surveillance for the whole horizon. Besides, the achieved performance is above the threshold as the actual estimation errors do not reach their (worst-case) maximum values. This is because we design the trajectories by considering the (worst-case) maximum possible errors. Moreover, the disguising achievements of the three sets of trajectories are compared. The developed method without bounds leads to a nearly indistinguishable disguising achievement to the randomized baseline. When the estimation errors are considered in the design, the disguising performance degrades slightly due to the reduced feasible solution space.

Another scenario with two nodes travelling on a closed road is considered. The moving nodes may represent some security guys patrolling a large asset, and they have to exchange sensing data in the mission. Here, $\Delta_{12}^u=10$ m, $\Delta_{21}^u=20$ m, $\Delta_{11}^n=20$ m, $\Delta_{12}^n=25$ m, $\Delta_{21}^n=10$ m and $\Delta_{22}^n=15$ m. All the other parameters keep the same as they are in the above case. The UAVs' trajectories are shown in Figs. 6a and 6b, where the estimation errors are not considered, and Figs. 6c and 6d when the error bounds are taken into account. The trajectories generated by the benchmark method are shown in Figs. 6e and 6f. The radio surveillance performance and disguising performance are shown in Figs. 6g and 6h, respectively. Similar to the first case, neither of the proposed method with no error bounds considered and the random method can ensure the radio surveillance performance to be

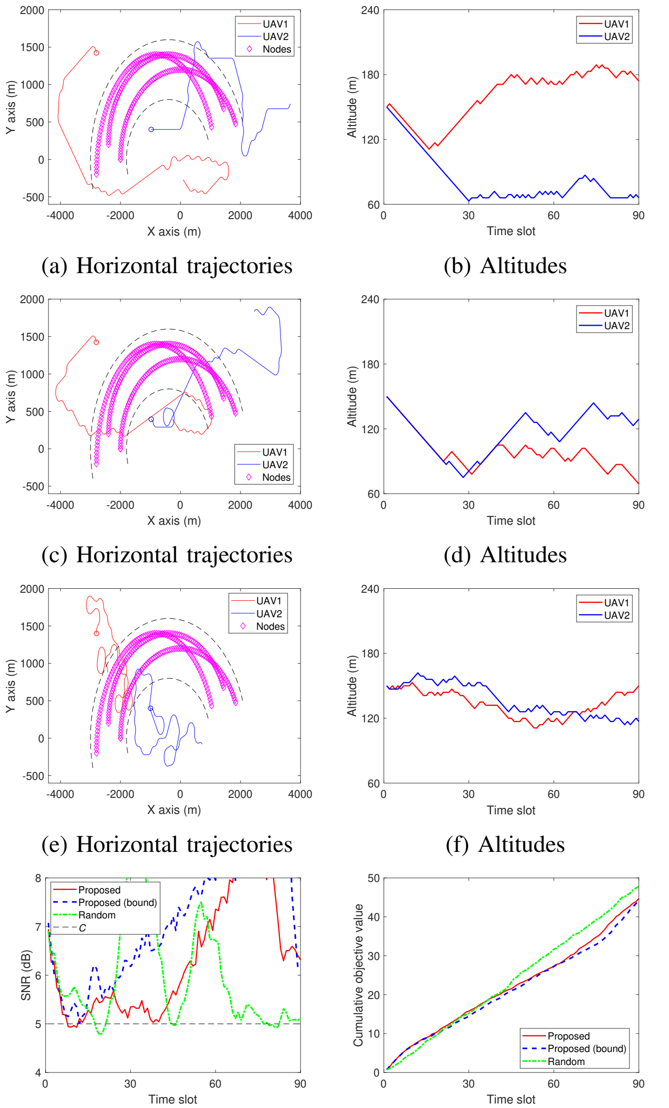

(a) Horizontal trajectories (b) Altitudes

(c) Horizontal trajectories (d) Altitudes

(e) Horizontal trajectories (f) Altitudes

(g) Eavesdropping performance (h) Disguising performance

Fig. 5: Case 1: Three moving nodes and two UAVs. (a-b) UAVs' trajectories with no error bounds considered. (c-d) UAVs' trajectories with error bounds considered. (e-f) UAVs' trajectories of the baseline. (g) Eavesdropping performance. (h) Disguising performance.

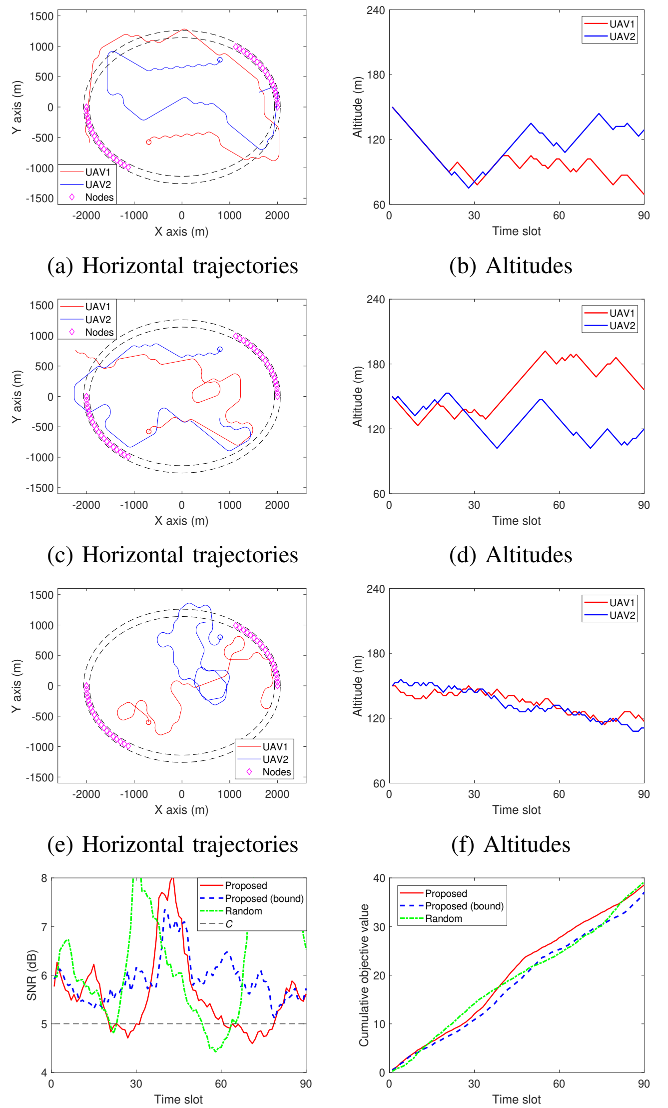

(a) Horizontal trajectories (b) Altitudes

(c) Horizontal trajectories (d) Altitudes

(e) Horizontal trajectories (f) Altitudes

(g) Eavesdropping performance (h) Disguising performance

Fig. 6: Case 1: Two moving nodes and two UAVs. (a-b) UAVs' trajectories with no error bounds considered. (c-d) UAVs' trajectories with error bounds considered. (e-f) UAVs' trajectories of the baseline. (g) Eavesdropping performance. (h) Disguising performance.

above the threshold C at any time. From the simulation results, we see that the proposed method considering the estimation error allows each UAV to construct its trajectory independently without sharing information. It guarantees the required radio surveillance performance (which cannot be guaranteed by the benchmark method) and achieves comparable disguising performances with the benchmark method.

Moreover, we add one more UAV to the above case. The parameters relating to this UAV are as follows. $S_3 = 120$ m, $\Delta^u_{13} = 10$ m, $\Delta^u_{23} = 20$ m, $\Delta^u_{31} = 15$ m, $\Delta^u_{32} = 15$ m, $\Delta^n_{31} = 10$ m and $\Delta^n_{32} = 10$ m. Other parameters are the same as above. The trajectories of the three UAVs by the developed approach considering the error bounds are shown in Fig. 7a, and their altitudes are shown in Fig. 7b. Fig. 7c shows the radio surveillance performance, which is above the threshold C at any time. Fig. 7d displays the cumulative disguising performance. Compared to the case of two UAVs, we see that the UAVs change their movement more drastically since having one more UAV reduces the workload on the other UAVs. The average disguising performance per UAV per node is about 11, while it is about 9 in the case of two UAVs (see Fig. 6h).

To demonstrate the scalability of the proposed algorithm, we consider different $\mathcal{N}$ and $\mathcal{M}$. We measure the execution time of the algorithm in MATLAB. We use a normal personal computer an Intel Core i7-7500U CPU. Other relevant parameters are the same as above. As seen from Fig. 8, with the increase of $\mathcal{M}$, the computing time of our method increases

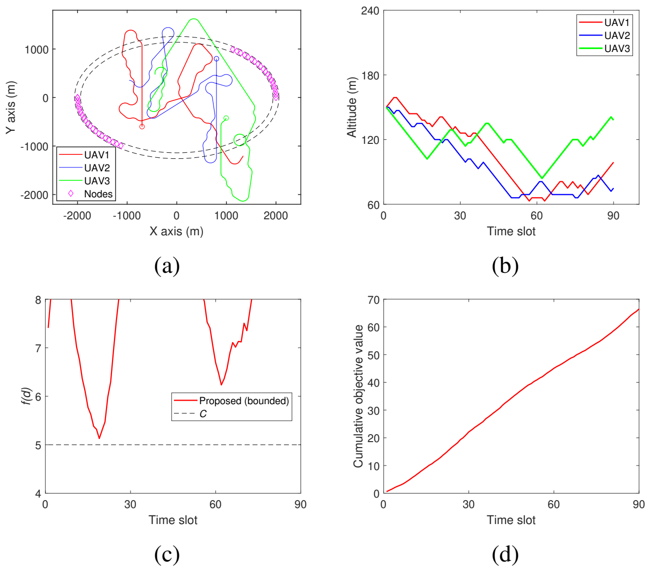

Fig. 7: Case 3: Two moving nodes and three UAVs. (a-b) UAVs' trajectories with no error bounds considered. (c) Eavesdropping performance. (d) Disguising performance.

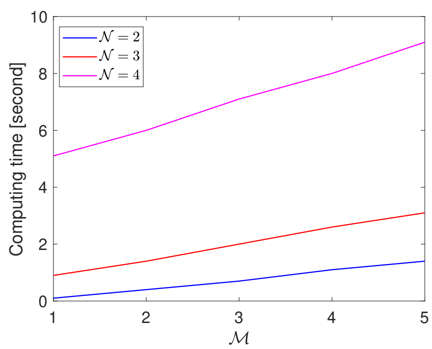

Fig. 8: The computing time of the proposed approach under various $\mathcal{M}$ and $\mathcal{N}$.

almost linearly. The computing time of the proposed algorithm increases significantly with $\mathcal{N}$. In this sense, the proposed algorithms scale well with the number of ground nodes $\mathcal{M}$.

In terms of efficiency, we evaluate numerically the number of floating-point operations of our method by using the MATLAB command, FLOPs[1]. Consider the case with three UAVs and two ground nodes. With the aforementioned parameters $\mathcal{L}$, n_v, n_μ and n_ϕ, the number of floating-point operations is about 0.3×10^6. Take an off-the-shelf UAV on-board computer, Qualcomm Snapdragon Flight [32, Tab. IV], for example, whose on-board computer has the computing capability of 167 GFLOPs (which can execute 167×10^9 floating-point operations per second). The proposed method can be implemented in real-time with the frequency of planning less than 1 Hz.

[1]https://www.mathworks.com/matlabcentral/fileexchange/50608-counting-the-floating-point-operations-flops

V. Concluding Remark

This paper considers the usage of a team of UAVs for monitoring a group of moving nodes collaboratively and secretively. To this end, the UAVs need to construct their trajectories online and decentralizedly. A measurement to describe the disguising performance of UAVs is adopted. The trajectory planning task is modelled as a constrained optimization problem. The objective is the maximization of the disguising metric, and the constraints include an instantaneous radio surveillance requirement, the requirement of avoiding collision, and the aeronautic manoeuvrability. A trajectory construction method based on MPC is presented to solve the problem online. The method tolerates inaccurate position estimations. Simulations have been conducted to evaluate the developed approach, and the results reveal that the developed approach ensures the instantaneous radio surveillance requirement on the targets, while not compromising the disguising purpose, as compared to a random method.

References

[1] K. Harikumar, J. Senthilnath, and S. Sundaram, "Multi-UAV oxyrrhis marina-inspired search and dynamic formation control for forest firefighting," *IEEE Transactions on Automation Science and Engineering*, vol. 16, no. 2, pp. 863–873, 2019.

[2] N. Mathew, S. L. Smith, and S. L. Waslander, "Planning paths for package delivery in heterogeneous multirobot teams," *IEEE Transactions on Automation Science and Engineering*, vol. 12, no. 4, pp. 1298–1308, 2015.

[3] P. Tokekar, J. V. Hook, D. Mulla, and V. Isler, "Sensor planning for a symbiotic UAV and UGV system for precision agriculture," *IEEE Transactions on Robotics*, vol. 32, no. 6, pp. 1498–1511, 2016.

[4] J. Li, T. Sun, X. Huang, L. Ma, Q. Lin, J. Chen, and V. C. M. Leung, "A memetic path planning algorithm for unmanned air/ground vehicle cooperative detection systems," *IEEE Transactions on Automation Science and Engineering*, pp. 1–14, 2021.

[5] X.-W. Tang, X.-L. Huang, and F. Hu, "QoE-Driven UAV-enabled pseudo-analog wireless video broadcast: A joint optimization of power and trajectory," *IEEE Transactions on Multimedia*, 2020.

[6] H. Huang and A. V. Savkin, "A method for optimized deployment of unmanned aerial vehicles for maximum coverage and minimum interference in cellular networks," *IEEE Transactions on Industrial Informatics*, vol. 15, no. 5, pp. 2638–2647, 2019.

[7] D. Ma, Y. Li, X. Hu, H. Zhang, and X. Xie, "An optimal three-dimensional drone layout method for maximum signal coverage and minimum interference in complex pipeline networks," *IEEE Transactions on Cybernetics*, pp. 1–9, 2020.

[8] D. Wang, B. Bai, G. Zhang, and Z. Han, "Optimal placement of low-altitude aerial base station for securing communications," *IEEE Wireless Communications Letters*, vol. 8, no. 3, pp. 869–872, 2019.

[9] M. Cui, G. Zhang, Q. Wu, and D. W. K. Ng, "Robust trajectory and transmit power design for secure UAV communications," *IEEE Transactions on Vehicular Technology*, vol. 67, no. 9, pp. 9042–9046, Sep. 2018.

[10] G. Zhang, Q. Wu, M. Cui, and R. Zhang, "Securing UAV communications via joint trajectory and power control," *IEEE Transactions on Wireless Communications*, vol. 18, no. 2, pp. 1376–1389, Feb 2019.

[11] Y. Zhou, P. L. Yeoh, H. Chen, Y. Li, R. Schober, L. Zhuo, and B. Vucetic, "Improving physical layer security via a UAV friendly jammer for unknown eavesdropper location," *IEEE Transactions on Vehicular Technology*, vol. 67, no. 11, pp. 11 280–11 284, Nov 2018.

[12] H. Lei, D. Wang, K. Park, I. S. Ansari, J. Jiang, G. Pan, and M. Alouini, "Safeguarding UAV IoT communication systems against randomly located eavesdroppers," *IEEE Internet of Things Journal*, vol. 7, no. 2, pp. 1230–1244, 2020.

[13] Q. Wang, Z. Chen, W. Mei, and J. Fang, "Improving physical layer security using UAV-enabled mobile relaying," *IEEE Wireless Communications Letters*, vol. 6, no. 3, pp. 310–313, June 2017.

[14] J. Guo, N. Zhao, Z. Yang, F. R. Yu, Y. Chen, and V. C. M. Leung, "Proactive jamming toward interference alignment networks: Beneficial and adversarial aspects," *IEEE Systems Journal*, vol. 13, no. 1, pp. 412–423, 2019.

[15] P. Chen, J. Ouyang, W. Zhu, M. Lin, A. E. Shafie, and N. Al-Dhahir, "Artificial-noise-aided energy-efficient secure beamforming for multi-eavesdroppers in cognitive radio networks," *IEEE Systems Journal*, pp. 1–12, 2020.

[16] A. Li, Q. Wu, and R. Zhang, "UAV-enabled cooperative jamming for improving secrecy of ground wiretap channel," *IEEE Wireless Communications Letters*, vol. 8, no. 1, pp. 181–184, 2019.

[17] H. Lee, S. Eom, J. Park, and I. Lee, "UAV-aided secure communications with cooperative jamming," *IEEE Transactions on Vehicular Technology*, vol. 67, no. 10, pp. 9385–9392, Oct 2018.

[18] Y. Cai, F. Cui, Q. Shi, M. Zhao, and G. Y. Li, "Dual-UAV-enabled secure communications: Joint trajectory design and user scheduling," *IEEE Journal on Selected Areas in Communications*, vol. 36, no. 9, pp. 1972–1985, Sep. 2018.

[19] Y. Li, R. Zhang, J. Zhang, and L. Yang, "Cooperative jamming via spectrum sharing for secure UAV communications," *IEEE Wireless Communications Letters*, pp. 1–1, 2020.

[20] H. Huang, A. V. Savkin, and W. Ni, "Online UAV trajectory planning for covert video surveillance of mobile targets," *IEEE Transactions on Automation Science and Engineering*, pp. 1–12, 2021.

[21] X. Yuan, Z. Feng, W. Ni, R. P. Liu, J. A. Zhang, and W. Xu, "Secrecy performance of terrestrial radio links under collaborative aerial eavesdropping," *IEEE Transactions on Information Forensics and Security*, vol. 15, pp. 604–619, 2020.

[22] A. V. Savkin and H. Huang, "A method for optimized deployment of a network of surveillance aerial drones," *IEEE Systems Journal*, vol. 13, no. 4, pp. 4474–4477, 2019.

[23] X.-L. Huang, X. Ma, and F. Hu, "Machine learning and intelligent communications," *Mobile Networks and Applications*, vol. 23, no. 1, pp. 68–70, 2018.

[24] A. V. Savkin, H. Huang, and W. Ni, "Securing UAV communication in the presence of stationary or mobile eavesdroppers via online 3D trajectory planning," *IEEE Wireless Communications Letters*, vol. 9, no. 8, pp. 1211 – 1215, 2020.

[25] H. Huang, A. V. Savkin, and W. Ni, "Navigation of a UAV team for collaborative eavesdropping on multiple ground transmitters," *IEEE Transactions on Vehicular Technology*, vol. 70, no. 10, pp. 10 450–10 460, 2021.

[26] ——, "Decentralized covert and collaborative radio surveillance on a group of mobile ground nodes by a UAV swarm," in *2020 IEEE 18th International Conference on Industrial Informatics (INDIN)*, vol. 1, 2020, pp. 307–310.

[27] I. Lugo-Cárdenas, S. Salazar, and R. Lozano, "Lyapunov Based 3D Path Following Kinematic Controller for a Fixed Wing UAV," *IFAC-PapersOnLine*, vol. 50, no. 1, pp. 15 946–15 951, 2017.

[28] Y. Zhang, Y. Shen, H. Wang, J. Yong, and X. Jiang, "On secure wireless communications for IoT under eavesdropper collusion," *IEEE Transactions on Automation Science and Engineering*, vol. 13, no. 3, pp. 1281–1293, 2016.

[29] D. Sikeridis, E. E. Tsiropoulou, M. Devetsikiotis, and S. Papavassiliou, "Wireless powered public safety IoT: A UAV-assisted adaptive-learning approach towards energy efficiency," *Journal of Network and Computer Applications*, vol. 123, pp. 69–79, 2018.

[30] P. N. Pathirana, A. V. Savkin, and S. Jha, "Location estimation and trajectory prediction for cellular networks with mobile base stations," *IEEE Transactions on Vehicular Technology*, vol. 53, no. 6, pp. 1903–1913, Nov 2004.

[31] A. N. Kolmogorov and S. V. Fomin, *Introductory real analysis*. New York: Dover, 1975.

[32] A. Bemporad, M. Morari, V. Dua, and E. N. Pistikopoulos, "The explicit linear quadratic regulator for constrained systems," *Automatica*, vol. 38, no. 1, pp. 3–20, 2002.

[33] A. Richards and J. How, "Robust stable model predictive control with constraint tightening," in *2006 American Control Conference*. IEEE, 2006, pp. 6–pp.

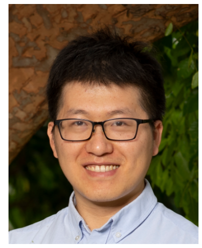

Hailong Huang received the B.Sc. degree in automation, from China University of Petroleum, Beijing, China, in 2012, and received Ph.D degree in Systems and Control from the University of New South Wales, Sydney, Australia, in 2018. He was a post-doctoral research fellow at the School of Electrical Engineering and Telecommunications, University of New South Wales, Sydney, Australia. He is now an Assistant Professor at the Department of Aeronautical and Aviation Engineering, the Hong Kong Polytechnic University, Hong Kong. His current research interests include guidance, navigation, and control of mobile robots, multi-agent systems, and distributed control.

Andrey V. Savkin was born in 1965 in Norilsk, Russia. He received the M.S. and Ph.D. degrees in mathematics from the Leningrad State University, Saint Petersburg, Russia, in 1987 and 1991, respectively. From 1987 to 1992, he was with the Television Research Institute, Leningrad, Russia. From 1992 to 1994, he held a Postdoctoral position in the Department of Electrical Engineering, Australian Defence Force Academy, Canberra. From 1994 to 1996, he was a Research Fellow in the Department of Electrical and Electronic Engineering and the Cooperative Research Centre for Sensor Signal and Information Processing, University of Melbourne, Australia. From 1996 to 2000, he was a Senior Lecturer, and then an Associate Professor in the Department of Electrical and Electronic Engineering, University of Western Australia, Perth. Since 2000, he has been a Professor in the School of Electrical Engineering and Telecommunications, University of New South Wales, Sydney, NSW, Australia. His current research interests include robust control and state estimation, hybrid dynamical systems, guidance, navigation and control of mobile robots, applications of control and signal processing in biomedical engineering and medicine. He has authored/coauthored seven research monographs and numerous journal and conference papers on these topics. Prof. Savkin has served as an Associate Editor for several international journals.

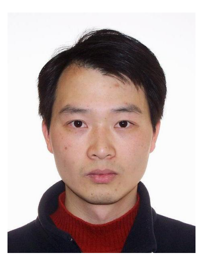

Wei Ni received the B.E. and Ph.D. degrees in Electronic Engineering from Fudan University, Shanghai, China, in 2000 and 2005, respectively. Currently, he is a Group Leader and Principal Research Scientist at CSIRO, Sydney, Australia, and an Adjunct Professor at the University of Technology Sydney and Honorary Professor at Macquarie University, Sydney. He was a Postdoctoral Research Fellow at Shanghai Jiaotong University from 2005–2008; Deputy Project Manager at the Bell Labs, Alcatel/Alcatel-Lucent from 2005 to 2008; and Senior Researcher at Devices R&D, Nokia, Shanghai, from 2008 to 2009. His research interests include signal processing, stochastic optimization, learning, as well as their applications to network efficiency and integrity.

Dr Ni is the Chair of IEEE Vehicular Technology Society (VTS) New South Wales (NSW) Chapter since 2020 and an Editor of IEEE Transactions on Wireless Communications since 2018. He served first the Secretary and then Vice-Chair of IEEE NSW VTS Chapter from 2015 to 2019, Track Chair for VTC-Spring 2017, Track Co-chair for IEEE VTC-Spring 2016, Publication Chair for BodyNet 2015, and Student Travel Grant Chair for WPMC 2014.